SOFiSTiK

Benchmark Example No. 48

Triaxial Consolidated Undrained (CU) Test

SOFiSTiK | 2022

VERiFiCATiON
BE48 Triaxial Consolidated Undrained (CU) Test

VERiFiCATiON Manual, Service Pack 2022-12 Build 74

SOFiSTiK AG

HQ Nuremberg
Flataustraße 14
90411 Nürnberg
Germany

T +49 (0)911 39901-0
F +49(0)911 397904

Office Garching
Parkring 2
85748 Garching bei München
Germany

T +49 (0)89 315878-0
F +49 (0)89 315878-23

info@sofistik.com
www.sofistik.com

Front Cover

Arnulfsteg, Munich Photo: Hans Gössing

Overview	
Element Type(s):	CAXI
Analysis Type(s):	MNL
Procedure(s):	LSTP
Topic(s):	SOIL
Module(s):	TALPA
Input file(s):	triaxial_cu_test.dat, triaxial_cu_test_200.dat

1 Problem Description

In this example a consolidated undrained (CU) triaxial test on a loose Hostun-RF sand is simulated. The specimen is subjected to different levels of triaxial confining stresses and the results are compared to those of the experimental tests and numerical simulations, as described in Wehnert [1].

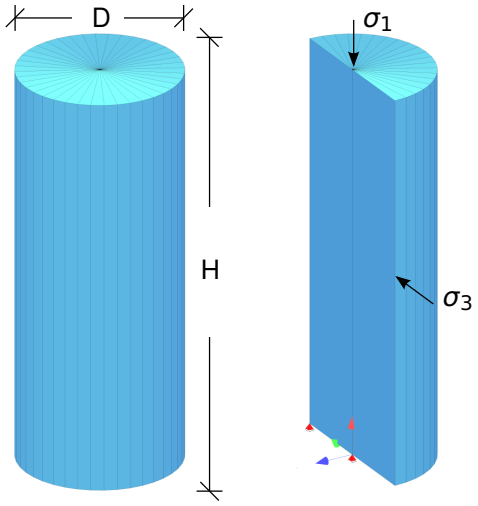

Figure 1: Problem Description

2 Reference Solution

In this example two soil models are utilised, the Mohr-Coulomb (MC) and the Hardening Soil (HS) model. Further details on these two models can be found in Benchmarks 20 and 21.

The choice of the appropriate model for the soil is of a significant importance. For example, MC model can significantly overestimate the undrained shear strength for a normally consolidated soil. More advanced models can provide better estimate for the undrained strength than the MC model. In particular, the HS model is able to represent the change of the excess pore water pressure occurring under undrained shear loading conditions, providing more realistic effective stress paths and values for undrained shear strength. However, the results of the analysis with the Hardening Soil model are very sensitive to the used model parameters and the choice of the dilatancy model. Therefore, in this example for the HS model different dilatancy formulations are tested and their influence on the result examined.

A well-established stress dilatancy theory is described by Rowe [2], where the so-called mobilized dilatancy angle ψ_m is defined as

$$\sin\psi_m = \frac{\sin\varphi_m - \sin\varphi_{cs}}{1 - \sin\varphi_m \sin\varphi_{cs}} \tag{1}$$

Therein, the critical state friction angle φ_{cs} marks the transition between contractive (small stress ratios with $\varphi_m < \varphi_{cs}$) and dilatant (higher stress ratios with $\varphi_m > \varphi_{cs}$) plastic flow. The mobilized friction angle φ_m in Equation 1 is computed according to

$$\sin\varphi_m = \frac{\sigma_1' - \sigma_3'}{2c \cdot \cot\varphi - \sigma_1' - \sigma_3'} \tag{2}$$

At failure, when $\varphi_m \equiv \varphi$, also the dilatancy angle reaches its final value $\psi_m \equiv \psi$. Accordingly, from Equation 1 the critical state friction angle can be derived as

$$\sin\varphi_{cs} = \frac{\sin\varphi - \sin\psi}{1 - \sin\varphi \sin\psi} \tag{3}$$

It has been recognized that in some cases the Rowe's model for dilatancy angles (Eq. 1) can overestimate the contractive behavior of the soil at low mobilized friction angles, $\varphi_m < \varphi_{cs}$. As a remedy, several researchers have developed modified formulations based on the original Rowe's model. Some of these models which are implemented in SOFiSTiK are described below.

One of the models which does not require additional input parameters is the model according to Soreide [3] which modifies the Rowe's formulation by using the scaling factor $\sin\varphi_m / \sin\varphi$

$$\sin\psi_m = \frac{\sin\varphi_m - \sin\varphi_{cs}}{1 - \sin\varphi_m \sin\varphi_{cs}} \cdot \frac{\sin\varphi_m}{\sin\varphi} \,. \tag{4}$$

Wehnert [1] proposed a model based on a lower cut-off value ψ_0 for the modification of the Rowe's formulation from Eq. 1 at low mobilized friction angles

$$\sin\psi_m = \begin{cases} \sin\psi_0 & ; \quad 0 < \psi_m \leq \psi_m^{Rowe} \\ \dfrac{\sin\varphi_m - \sin\varphi_{cs}}{1 - \sin\varphi_m \sin\varphi_{cs}} & ; \quad \psi_m^{Rowe} < \psi_m \leq \psi \end{cases} . \tag{5}$$

This dilatancy model obviously requires a specification of an additional parameter, ψ_0.

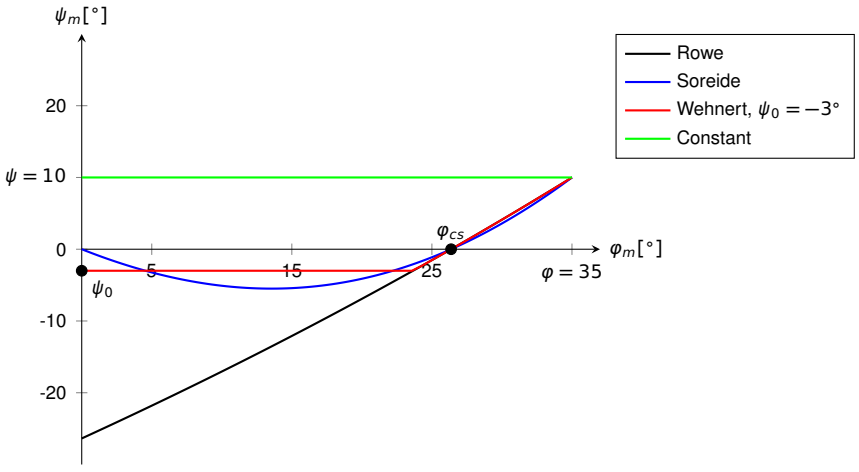

Figure 2: Comparison of models for mobilized dilatancy angle ψ_m implemented in SOFiSTiK for $\varphi = 35°$ and $\psi = 10°$

3 Model and Results

The properties of the model are presented in Table 1. Two material models are considered: the Mohr-Coulomb and the Hardening Soil, which is combined with the different dilatancy models as described by the formulations presented in Section 2. For the model according to Wehnert (Eq. 5) additional parameter, dilatancy ψ_0 at low stress ratios, is used. The undrained calculation is conducted in the form of effective stresses with effective shear parameters (c', φ') and stiffness parameters. Skempton's parameter $B \approx 0.9832$ (corresponding undrained Poisson's ratio is $\nu_u = 0.495$) is considered to describe the incompressibility of the pore water and saturated soil [1].

The analysis is carried out using an axisymmetric model. Two confining stress levels are considered, $\sigma_c = 200$ and $300\ kPa$. The undrained triaxial test on loose Hostun-RF sand is used as a reference. More information about the Hostun-RF sand can be found in Wehnert [1].

Table 1: Model Properties

Material		Geometry	Loading
$E = 60.0\ MN/m^2$	$E_{s,ref} = 16.0\ MN/m^2$	$H = 0.09\ m$	Phase I:
$\nu_{ur} = 0.25$	$E_{50,ref} = 12.0\ MN/m^2$	$D = 0.036\ m$	$\sigma_1 = \sigma_3 = \sigma_c =$
$\gamma = 0.0\ MN/m^3$	$m = 0.75$		$= 200, 300\ kPa$
$c' = 0.01\ kN/m^2$	$R_f = 0.9$		Phase II:
$\varphi' = 34°$	$K_0 = 0.44$		$\sigma_3 = \sigma_c = 200, 300\ kPa$
$\psi = 2°$	$B = 0.9832$		$\sigma_1 = \sigma_a > \sigma_c$
$\psi_0 = -4°$			

The results, as calculated by SOFiSTiK, are presented in Figures 3 - 9 (MC, HS-Rowe, HS-Cons, HS-Soreide and HS-Wehnert). Figures 3 - 8, also include the results of the numerical simulations and of the experimental tests from Wehnert [1] (Wehnert, Exp. 1 and Exp. 2). On a $p - q$ diagram, apart from the effective stress paths (ESP), the total stress paths (TSP) as well as the Mohr-Coulomb failure condition (MC failure) based on the used shear parameters, c' and φ', are displayed.

First the numerical simulation results by Wehnert [1] are compared to the results from the laboratory tests (Exp. 1 and Exp. 2). Although the oedometer and the drained triaxial tests (see also Benchmark 49) show good agreement with the results from the laboratory tests, the results from the undrained triaxial tests show deviation from the experimental results (see Figs. 3 - 8)[1]. The difference comes mainly as a result of the used dilatancy model (Eq. 5) and the choice of the model parameters, i.e. the peak dilatancy angle ψ and the lower cut-off dilatancy angle ψ_0.

Comparing the results of the development of the deviatoric stress q and the excess pore water pressure p_{we} between the experiment and the calculation, one can notice a considerable difference, both for the confining stress level of $200\ kPa$ as well as for the level of $300\ kPa$ (Figs. 4, 5, 7 and 8). As explained in [1], the test sample with confining stress of $200\ kPa$ behaves significantly more dilatant than the sample with the confining stress of $300\ kPa$. Since only one material model has been used to model the soil, only one peak dilatancy angle can be used to represent the dilatancy effects of both test cases. This peak dilatancy angle of $\psi = 2°$ represents therefore a compromise, leading to a underestimation of the results for a test with a smaller confining stress level and to overestimation of the results with larger

[1] Note also that the experimental test results for different samples of the same soil deviate significantly from each other.

confining stress level at higher mobilized friction angels.

Further differences arise from the chosen dilatancy model and the used lower cut-off dilatancy angle $\psi_0 = -4°$[2]. Due to the presence of the negative mobilized dilatancy angle ($\psi_m < 0$) at low stress levels, the soil has the tendency to decrease its volume (contraction) under increase of the deviatoric stress q (shear). However, since the soil is under undrained conditions, the volumetric strains cannot develop, and as a result the excess pore pressure increases under shear. The increase of the excess pore pressure means that the effective stresses will reduce (ESP lines curve to the left in the $p-q$ plot, Figs. 3 and 6). With the increase of the stress level, the contractive behavior turns to dilatant, meaning that the negative rate of excess pore pressures (pore water under-pressure) will arise, excess pore pressures decrease and hence the effective stresses increase. This transition from contractant to dilatant behavior occurs when the mobilized friction angle φ'_m becomes larger than the phase transition angle φ'_f which is approximately equal to the critical state friction angle φ'_{cs} (see Fig. 2). As further noted by Wehnert [1], due to the fact that mobilized dilatancy angle at low stress levels is slightly heigher and kept constant ($\psi_m = \psi_0$ for $0 \leq \psi_m \leq \psi_m^{Rowe}$, Eq. 5), the pore water under-pressures are overestimated.

Next the SOFiSTiK results obtained using the same soil model and dilatancy formulation as in [1] (HS-Wehnert) can be compared with the reference numerical simulation results (Wehnert). They show good agreement.

Finally, in other to illustrate the effect that the chosen dilatancy model can have on the results of the undrained soil, the results of the computation using the hardening soil model with different dilatancy formulations from Section 2 are included.

3.1 Hostun-RF Sand, $\sigma_c = 200\ kN/m^2$

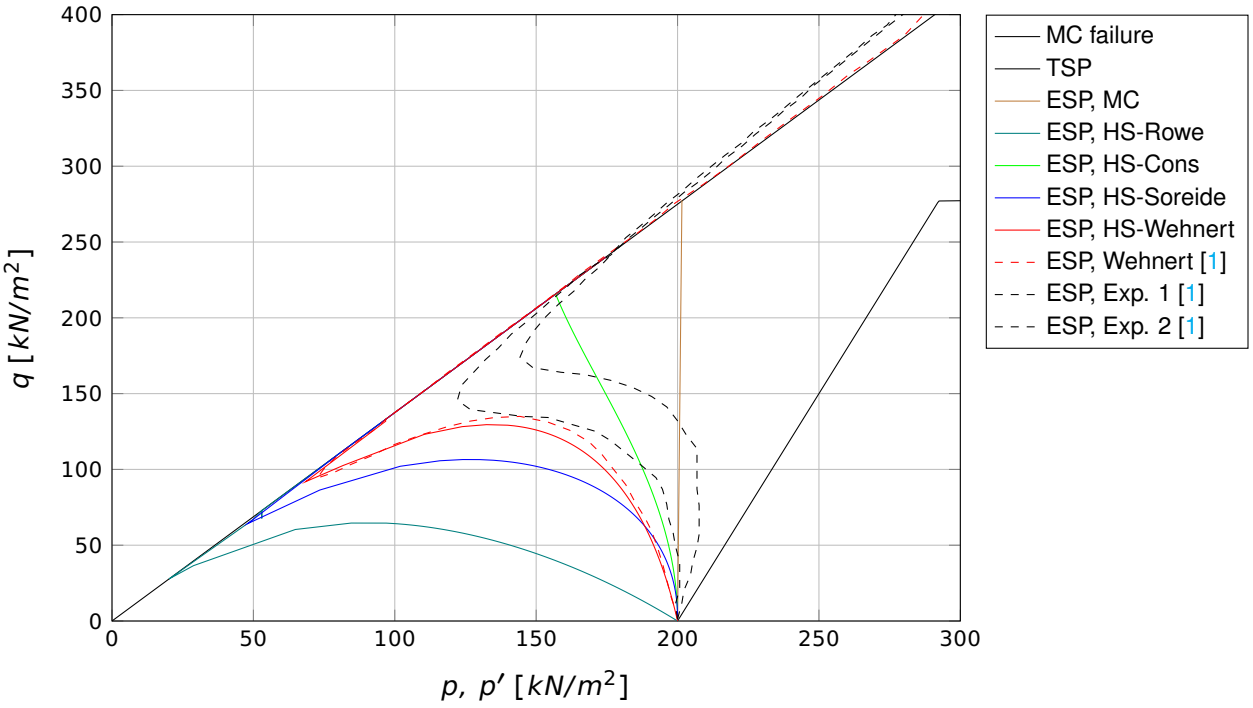

Figure 3: Effective stress path curve (q-p)

[2]The used value $\psi_0 = -4°$ is much higher than the values obtained from experimental tests, which range from $-13°$ to $-21°$. The reason for choosing this higher value is due to the fact that the experimental test used to obtain the dilatancy parameters involve not only shear but also some normal stress application to the test samples [1].

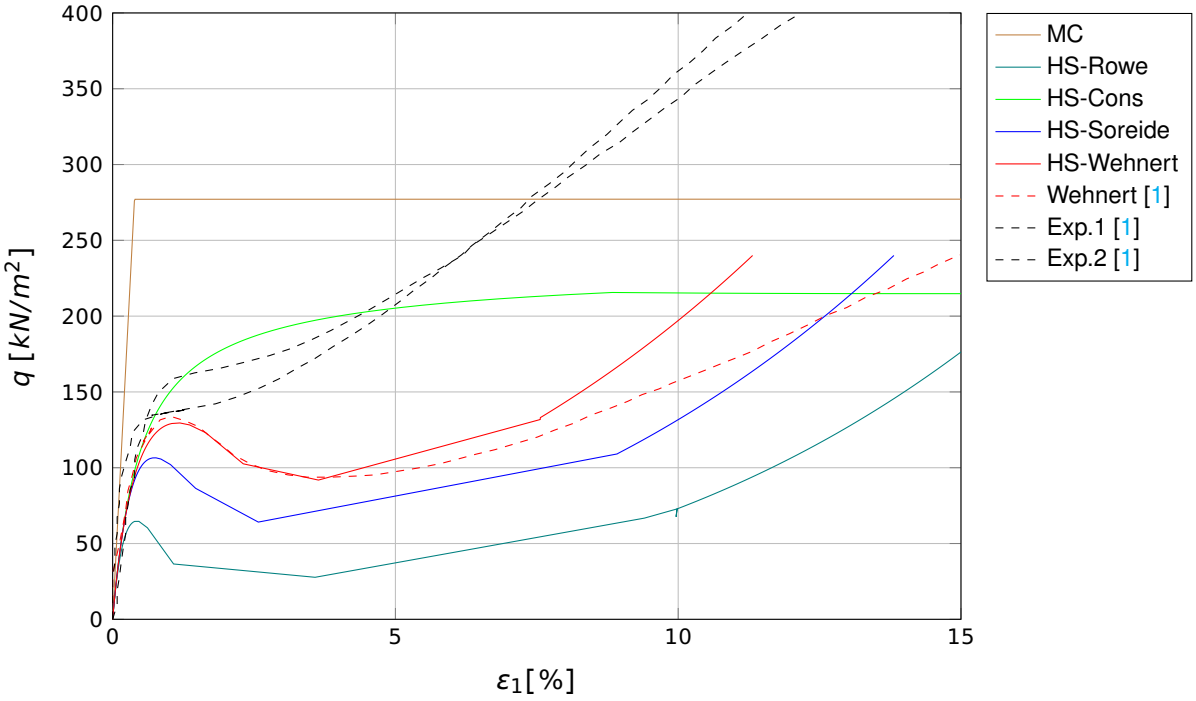

Figure 4: Deviatoric stress - axial strain curve (q-ε_1)

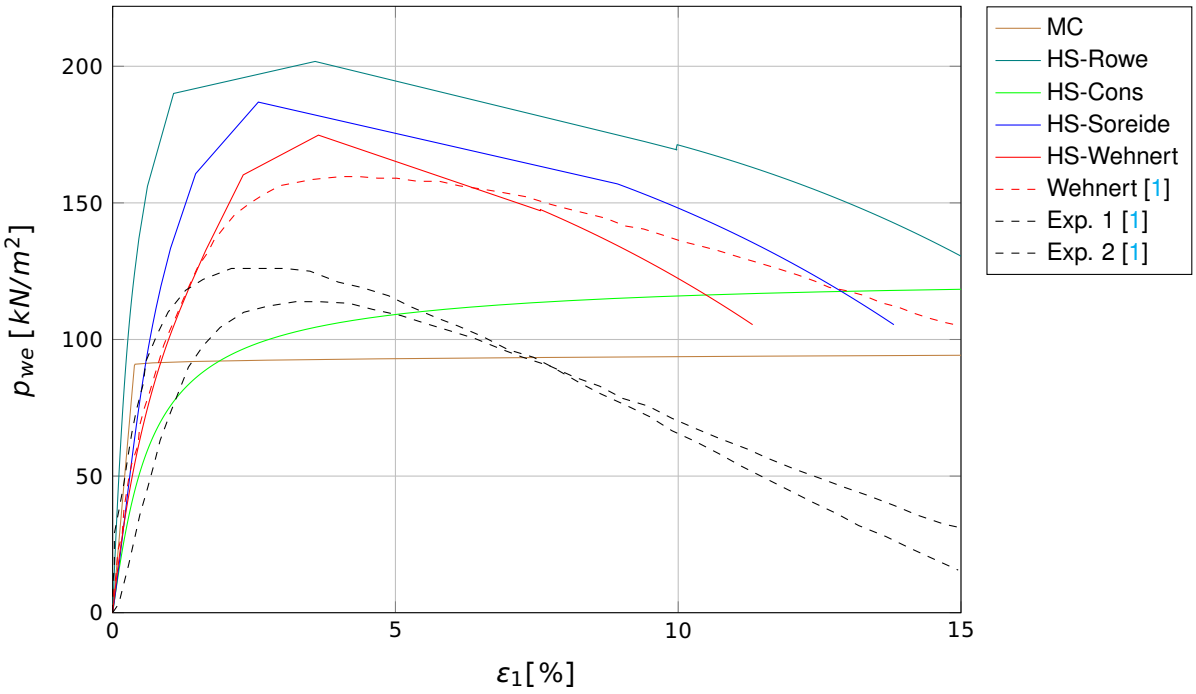

Figure 5: Excess porewater pressure - axial strain curve (p_{we}-ε_1)

3.2 Hostun-RF Sand, $\sigma_c = 300\ kN/m^2$

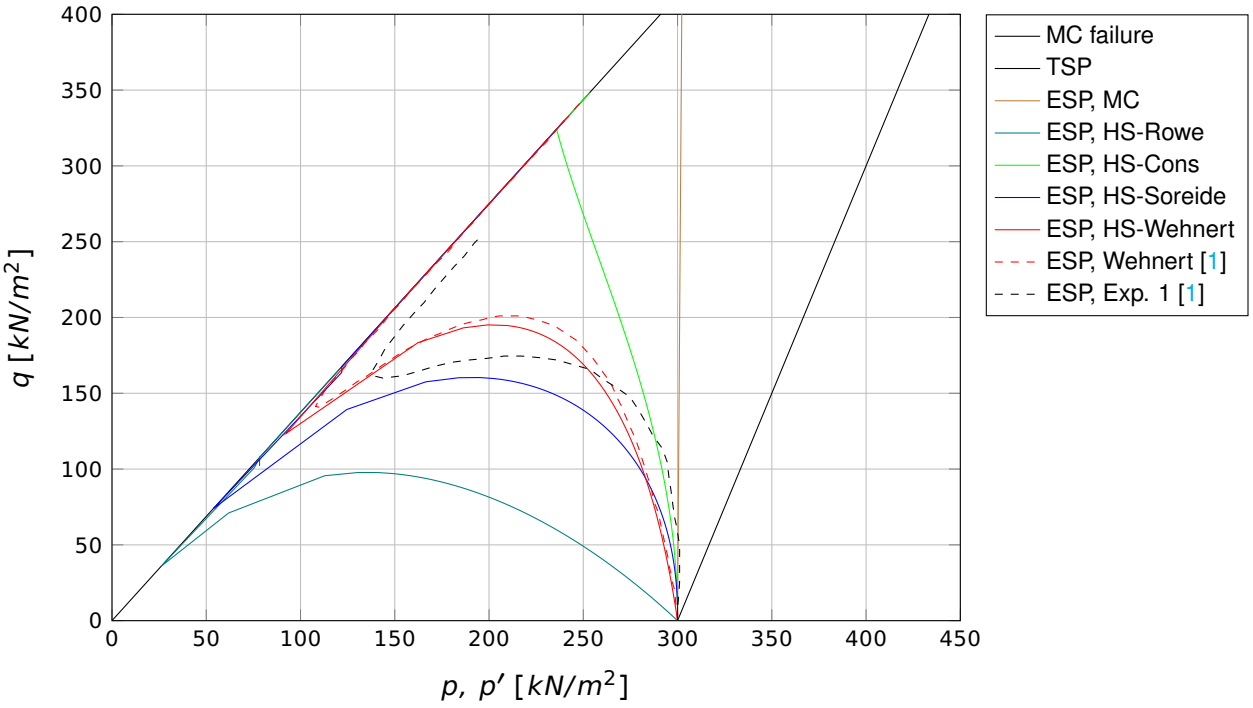

Figure 6: Effective stress path curve (q-p)

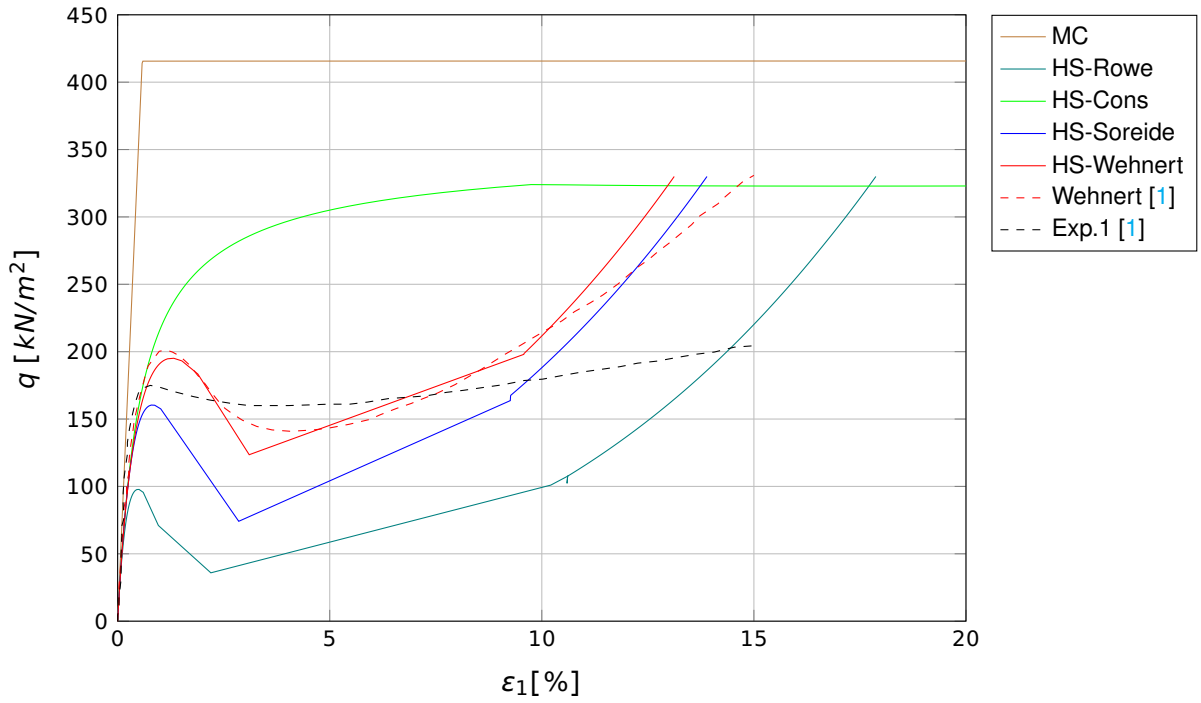

Figure 7: Deviatoric stress - axial strain curve (q-ε_1)

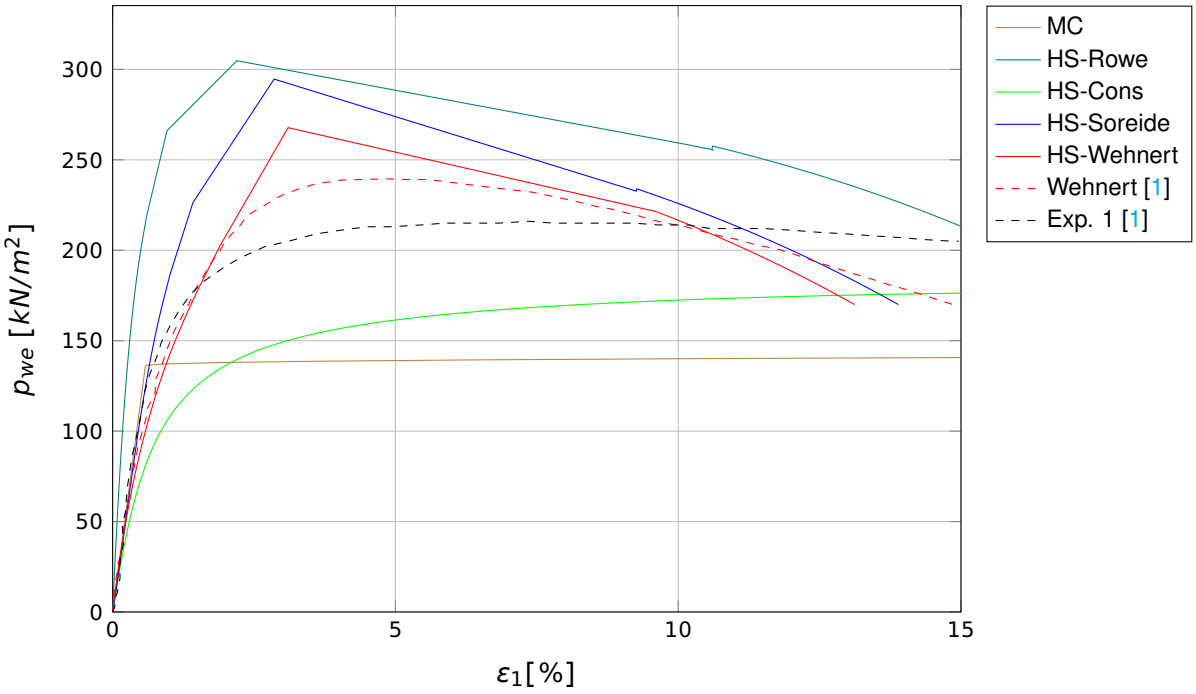

Figure 8: Excess porewater pressure - axial strain curve (p_{we}-ε_1)

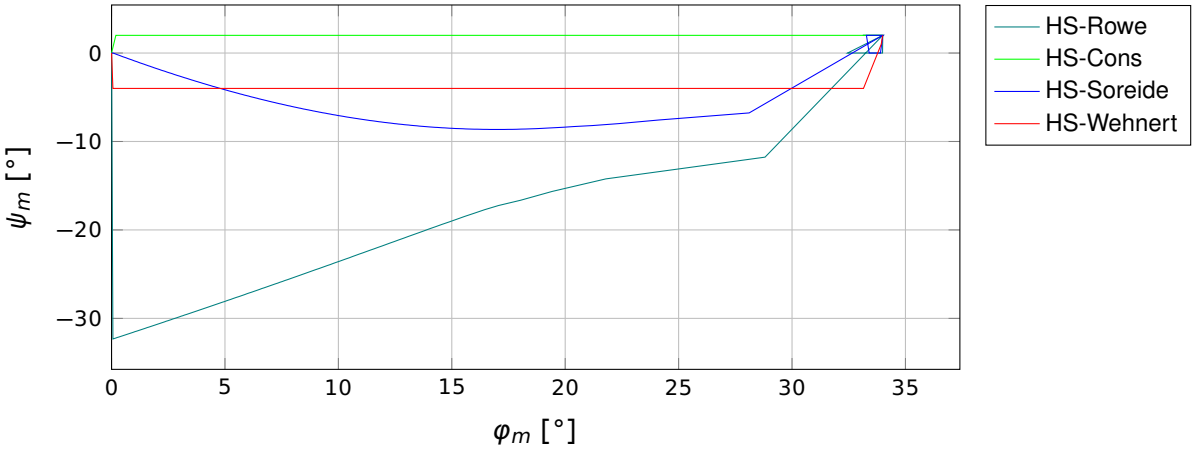

Figure 9: Mobilised dilatancy angle - friction angle curve (ψ_m-φ_m)

4 Conclusion

This example concerning the consolidated undrained triaxial test of a loose sand soil verifies that the Hardening Soil material model in combination with an appropriate choice of model parameters and dilatancy model is able to capture important behavior characteristics of the undrained soil. The numerical results are in a good agreement with the reference solution provided by Wehnert [1].

5 Literature

[1] M. Wehnert. *Ein Beistrag zur dreainerten und undrainerten Analyse in der Geotechnik.* Institut für Geotechnik, Universität Stuttgart: P. A. Vermeer, 2006.

[2] P.W. Rowe. “The stress-dilatancy relation for static equilibrium of an assembly of particles in contact”. In: *Proceedings of the Royal Society of London. Series A. Mathematical and Physical Sciences* 269.1339 (1962), pp. 500–527.

[3] O. K. Soreide. “Mixed hardening models for frictional soils”. PhD thesis. NTNU Norges teknisk-naturvitenskapelige universitet, 2003.